AIAA 98-3638

OPTICAL OSCILLATIONS IN A HALL THRUSTER

K. KOMURASAKI,
Y. SAKURAI,
and
D. KUSAMOTO

Nagoya University
Nagoya, Japan

34th AIAA/ASME/SAE/ASEE
Joint Propulsion Conference & Exhibit
July 13-15, 1998 / Cleveland, OH

AIAA 98-3638

OPTICAL OSCILLATIONS IN A HALL THRUSTER

Kimiya KOMURASAKI, Yasuyuki SAKURAI, and Daisuke KUSAMOTO
Department of Aerospace Engineering, Nagoya University
Chikusa, Nagoya 464-01, Japan

Abstract

Plasma oscillations in a Hall thruster were experimentally investigated by means of optical diagnostics. Optical emission from the discharge plasma in an acceleration channel was picked up through optical holes aligned axially and azimuthaly on a channel insulator. From the measured emission intensity oscillations, plasma perturbations were found to be propagating in the axial and azimuthal directions in the channel. There was no phase correlation between the azimuthal wave oscillations and discharge current oscillations, though the phase velocity had been closely related to the electron $E \times B$ drift motions. The perturbation observed in the axial direction thought to be one of the cause of discharge current oscillations.

Introduction

A great deal of researches have been focused on the lifetime and performance issues of Hall thrusters. Although the nominal performance of the Hall thruster has become reliable, there are still some phenomena being not clearly understood yet. One of these phenomena is the plasma oscillation. [1-8]

Plasma oscillations have been observed in the wide range of operational conditions. They can be classified into five regions such as

1) ionization oscillation (10 - 100 KHz),
2) transit-time oscillation (100 KHz - 1 MHz),
3) electron-drift oscillation (1-10 MHz),
4) Langmuir oscillation (100 MHz - 1 GHz), and
5) electron-cyclotron oscillation (1 GHz -).

Among these types of oscillation, low frequency ionization oscillations would be one of the main obstacles for improving its thrust efficiency. Although several discharge models are proposed, there is no adequate theory up to date, to describe these phenomena, and the relationship between oscillation and performance is still unknown.

In our previous researches,[9,10] it was found that the channel length is one of the most important design parameters which determine the thruster performance. With the shorter channel-length, the efficiency became higher but the discharge became unstable. The operational difficulty with the short channel-length thruster or the anode layer type thruster might be overcome by understanding the plasma dynamics in the channel. In this paper, the plasma oscillation in the acceleration channel was examined by means of optical diagnosis.

Experimental apparatus

Hall Thruster

A channel-length variable Hall thruster used in this study is schematically shown in Fig. 1. It has an acceleration channel insulated with two ceramic cylinders. The inner and outer diameter of the channel are 52 mm and 72 mm, respectively. The channel length is variable from 3 mm to 17 mm by changing anode-ring width. The anode is located at the upstream end of the channel and has twenty small apertures to uniformly feed the propellant gas into the channel. A solenoidal coil is set at the center of the thruster to apply magnetic fields in the radial direction in the channel. Magnetic induction is variable by changing the coil current and the maximum induction was approximately 0.08 T. The magnetic induction is distributed almost uniformly through the channel. This magnetic field configuration is basically different from that of SPT-type thrusters, whose magnetic induction distribution has a peak at the channel exit.

Xenon and argon are tested as a propellant gas. Propellant massflow rate is regulated using a thermal massflow controller. A filament cathode, which supplies electrons to sustain the discharge and to neutralize the ions, is used instead of a hollow cathode for operational convenience. The filament is made of 2% thoriated tungsten wires coated with the triple-carbonate powder to reduce its work function for electron emission.

Figure 2 shows a discharge characteristics of the thruster. It has a knee point, at which the propellant utilization approaches to 100 %.

Test Facility

All the measurements were performed in a vacuum chamber, which is 1.0 m in diameter and 1.6 m in length. It is evacuated by two diffusion pumps rated at 5000 l/s

each backed by a roots blower and a rotary pump. The background pressure is maintained in the order or 10^{-4} Torr during the operation. A schematic of the experimental setup is shown in Fig. 3. Three power supplies are used for main discharge, solenoidal-coil excitation and cathode heating. In order to stabilize the discharge, 20 Ω resistor is added to the main discharge circuit. It takes a few minutes for the main discharge to be stabilized.

Optical Diagnostics system

There are four optical-pickup holes on the outer insulator of the channel. The hole diameter is 1.0 mm. Ports #1, #2, and #3 are aligned in the axial direction. Port #1 is located at the position 9 mm upstream from the channel exit, and #2 and #3 are at 6 mm and 3 mm from the exit, respectively. When the channel length is 11 mm, Port #1 lies in the vicinity of the anode.

Ports #1 and #4 are aligned in the azimuthal direction with the phase difference of 90 degrees. A schematic of the acceleration channel and the optical pickups are shown in Fig. 4.

The emission from the discharge plasma is detected by photo-diodes (TOSHIBA, TPS708) at the outside of vacuum chamber through optical fibers. The photo-diodes are most sensitive at a wavelength of 820 nm and the sensitivity drops to 20% of that at 450 nm. The emission intensity signals are recorded simultaneously with the discharge current and voltage oscillations using a YOKOGAWA eight-channel digital oscilloscope. A multi-mode type optical fiber (MITSUBISHI DENSEN, Inc. STU800G-SY) with a large core diameter (800 μm) is used to minimize a transfer loss. The fibers are connected to a half depth of the pickup holes of the thruster.

Results and discussions

Discharge Oscillation

Typical discharge current oscillations are shown in Fig. 5. Owing to the irregular shape of the oscillation profiles, it was difficult to have a characteristic oscillation frequency from FFT analyses. Therefore, it was deduced from the averaged period of oscillations. As a result, the frequency ranged from 10~20 kHz and 400~500 kHz.

The ratio of fluctuated component of the discharge current to the averaged one is plotted in Fig. 6. It increased with the discharge current, especially beyond the knee point. Further increase in discharge current brought sudden break-down of the discharge.

To examine the influence of the electric circuit of a main-discharge power supply on the oscillation phenomena observed in the thruster, a KIKUSUI current-voltage regulated power supply and a laboratory made power supply were tested. The resulting trends were much the same for both power supplies.

Emission intensity oscillations in a channel

The FFT data of the emission intensity oscillations picked up at Port #1 (positioned at 2 mm from the anode) are presented in Fig. 7. In this case, a clear peak frequency is obtained from the FFT analyses.

Since the emission from the xenon neutrals, Xe I is stronger than that from xenon ions, Xe II, the emission intensity is roughly thought to indicate the number density of excited xenon neutrals.

The correlation between emission oscillation frequency and discharge voltage is shown in Fig. 8. The frequency ranged from 10 to 80 kHz at the discharge voltage of 60~170 V, and a linear relationship was observed between the oscillation frequency and discharge voltage.

There was no phase correlation between this emission oscillation and the discharge current oscillation simultaneously recorded. In addition, the oscillation frequencies also slightly differ from each other.

Plasma waves in the azimuthal direction

The phase difference between the emission intensity oscillations observed at Ports #1 and 4 are shown in Fig. 9. It indicates that the plasma wave is propagating in the azimuthal direction in the channel.

This azimuthal plasma wave is supposed to be closely related to the azimuthal electron motion caused by the interaction between the axial electric field, E and radial magnetic field, B. ($E \times B$ drift.)

The correlation between the measured phase velocity and the estimated E×B drift velocity is plotted in Fig. 10. The $E \times B$ drift velocity, V_d was estimated as

$$V_d = E / B \qquad (1)$$

Here, axial electric field was obtained from the measured plasma potential at the channel exit, ϕ_{exit} as

$$E = (\phi_{anode} - \phi_{exit}) / L \qquad (2)$$

where, ϕ_{anode} is the anode potential and L the channel length. Magnetic induction, B was measured using a Gauss-meter without the discharge.

Although the measured phase velocity is approximately half of the estimated E×B drift velocity, the linear correlation indicates the close relationship between the azimuthal wave and the electron drift.

The ion saturation current has also been measured at Ports #1 and #4 by using a single Langmuir probes. Phase velocity of the saturation-current oscillation is

plotted in Fig. 11. It shows a good coincidence with the phase velocity deduced from the emission intensity oscillation. Therefore, this azimuthal wave is though to be accompanied by density perturbations. The inhomogenous plasma density distribution could induce abnormal electron diffusion in the axial direction in the channel, resulting in poor acceleration efficiency of the Hall thruster discharge.

Plasma wave in the axial direction

Discharge oscillations are thought to be associated with the temporal variation of the plasma properties in the axial direction, not with the azimuthal variations. Figure 12 shows the emission intensity oscillations measured at Ports #1, #2 and #3, which are aligned in the axial direction.

Although there seems no phase difference in the axial direction in Fig. 12, there exists a little phase difference between the measured signals as shown in Fig. 13, which shows the intensity variations accumulated for 10 μs at the discharge current of 1.4 A. (At 1.4 A, the emission intensities at Ports #1 and #2 are almost compatible.) The maximum intensity has been observed at the Port #1 at t =20~70 μs, and at Port #2 otherwise.

The position of the maximum emission intensity is continuously shifting back and forth in the axial direction in the channel. This measured temporal change of the maximum-intensity position indicates that the portion where the ionization reaction is most vigorous is shifting in the axial direction in the channel.

As seen in the figures, it was difficult to separate the axial perturbation frequency from the azimuthal one because of the strong emission from the azimuthal perturbation. Therefore, the axial oscillation frequency has not been identified yet. However, it can be said that the axial oscillation frequency lies very close to the azimuthal oscillation frequency, and also to the discharge oscillation frequency in this series of experiments.

Summary

The emission-intensity oscillations in a Hall thruster were investigated by using optical fibers and photo-diodes. The results indicate that the plasma perturbations in the acceleration channel contain plasma waves propagating in the axial and azimuthal directions.

The characteristic of the azimuthal-wave phase velocity shows the close relationship between the azimuthal wave and the electron $E \times B$ drift. The inhomogenous density distribution caused by this wave would induce abnormal electron diffusion in the channel.

The observed axial emission-intensity perturbation indicates that the portion where ionization reaction is most vigorous is shifting back and forth in the channel. This might be associated with the discharge current oscillations of the thruster.

References

1) Baranov V.I., Nazarenko Y.S., Petrosov V.A., Vasin A.I., Yashnov Y.M., "Theory of Oscillations and Conductivity for Hall Thruster," 32nd Joint Propulsion Conf., AIAA Paper 96-3192, FL, July, 1996.

2) Baranov V.I., Nazarenko Y.S., Petrosov V.A., Vasin A.I., Yashnov Y.M., "The ionization oscillations mechanism in ACD", 24th Int'l Electric Propulsion Conf., Moscow, IEPC-95-37 (1995).

3) Hamley J.A., Sankovic J.M., Petrenko A.N., Manzella D.H., Cartier K.C., "The effect of power supply output characteristics on the operation of the SPT-100 thruster", 24th Int'l Electric Propulsion Conf., Moscow, IEPC-95-241 (1995).

4) Baranov V.I., Nazarenko Y.S., Petrosov V.A., Vasin A.I., Yashnov Y.M., "New conception of oscillation mechanisms in the accelerators with closed drift of electrons", 24th Int'l Electric Propulsion Conf., Moscow, IEPC-95-44 (1995).

5) Baranov V.I., Nazarenko Y.S., Petrosov V.A., Vasin A.I., Yashnov Y.M., "Electron drift oscillations outside acceleration zone of accelerator with closed electron drift", 24th Int'l Electric Propulsion Conf., Moscow, IEPC-95-62 (1995).

6) Fife J.M., and Martinez-Sanchez M.," Comparison of Results from a Two-Dimensional Numerical SPT Model with Experiment," 32nd Joint Propulsion Conf., AIAA Paper 96-3197, FL, July, 1996.

7) Kusamoto D., and Komurasaki K., "Optical Diagnosis of Plasma in a Channel of Hall Thrusters," 25th Int'l Electric Propulsion Conf., Cleveland, OH, IEPC-97-067 (1997).

8) Fife J.M., Martinez-Sanchez M., and Szabo, J., "A Numerical Study of Low Frequency Discharge Oscillations in Hall Thrusters," 33rd Joint Propulsion Conference, AIAA Paper 97-3052, WA, July, 1997.

9) Komurasaki, K., Mikami, K., and Fujiwara, T., "Optimization of Channel Configuration of Hall Thrusters, " Proc. 24th Intl. Electric Propulsion Conf., Moscow (1995),pp. 270-276.

10) Komurasaki K., Mikami K., and Kusamoto D., "Channel Length and Thruster Performance of Hall Thrusters," 32nd Joint Propulsion Conf., AIAA Paper 96-3194, FL, July, 1996.

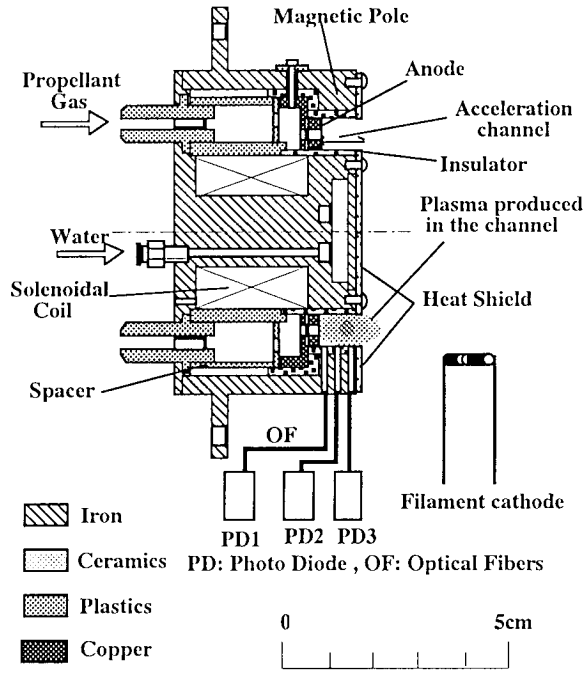

Fig. 1 Nagoya University Hall Thruster

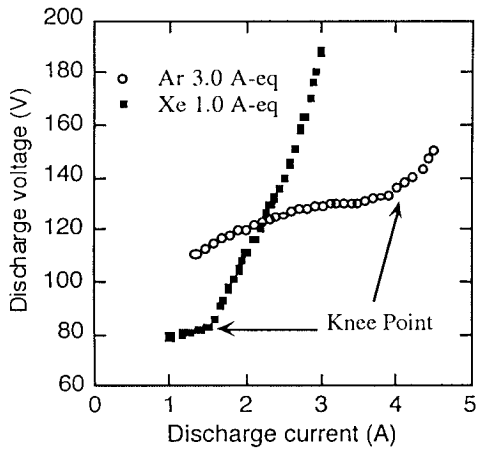

Fig. 2 Discharge characteristics

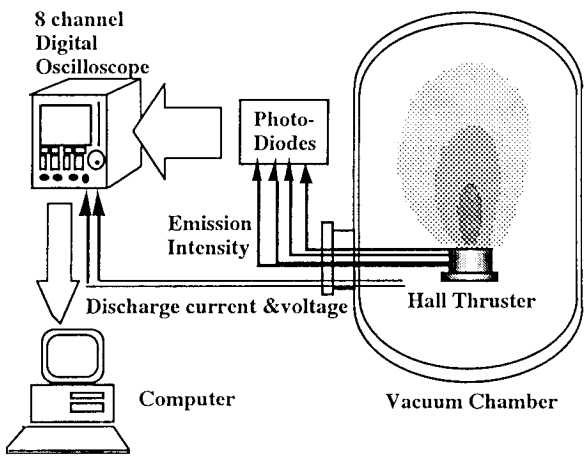

Fig. 3 Experimental setup.

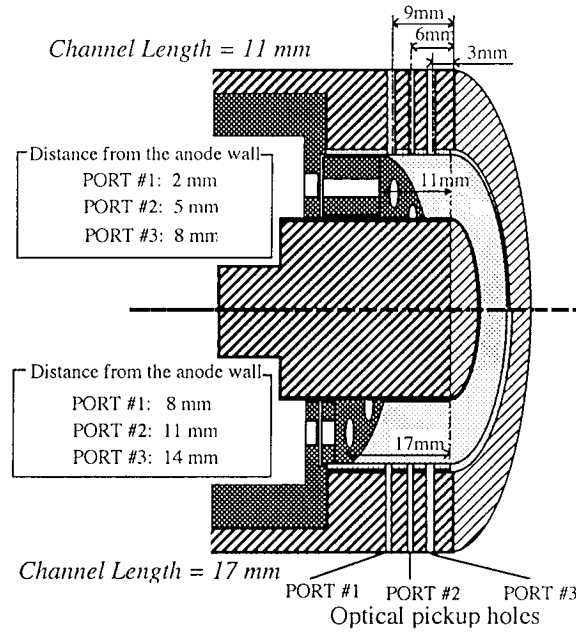

Fig. 4 An acceleration channel and optical pickups.

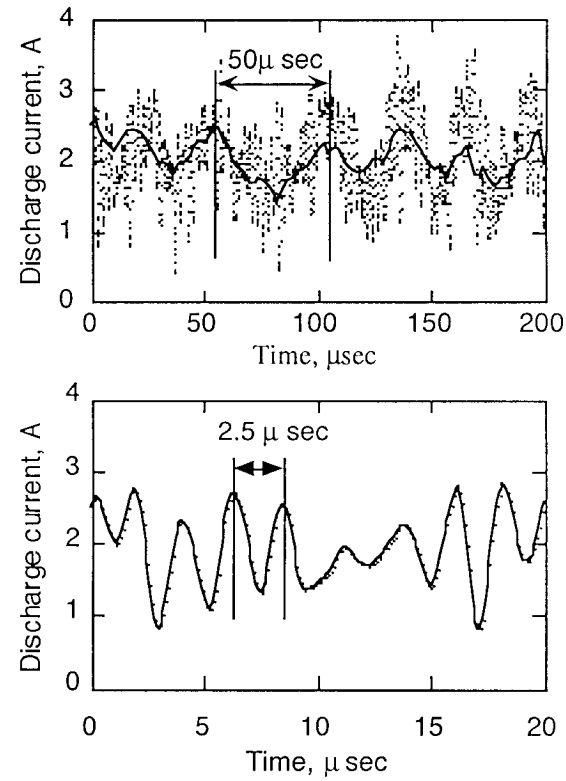

Fig. 5 Discharge current oscillations in different time scales.

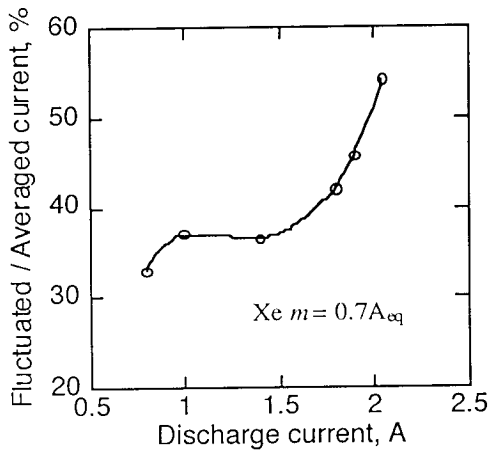

Fig. 6 Amplitude of the discharge current oscillation. B = 0.08 T.

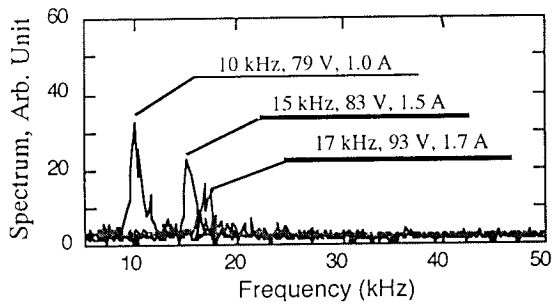

Fig. 7 FFT data of the emission intensity oscillations. B = 0.08 T, xenon 1.0 Aeq.

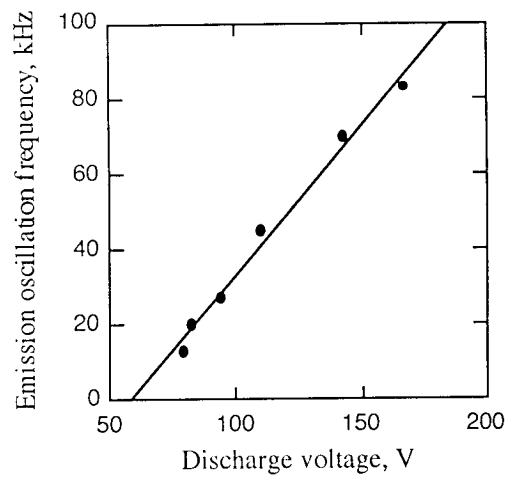

Fig. 8 Correlation between emission-intensity oscillation frequency and discharge voltage. B = 0.08 T, xenon 1.0 Aeq.

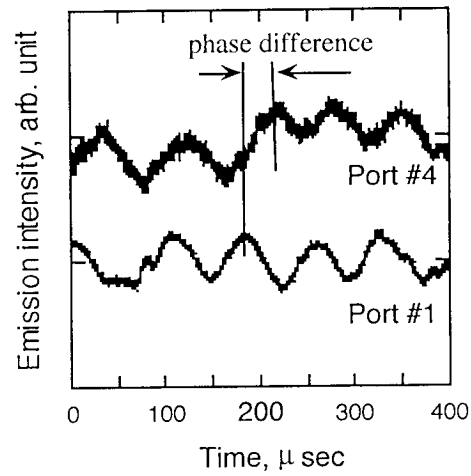

Fig. 9 Emission intensity oscillations measured at Ports #1 and #4 (aligned in the azimuthal direction.)

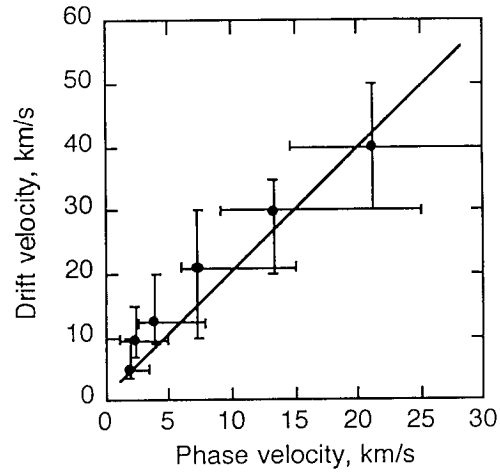

Fig. 10 Correlation between phase velocity and E×B drift velocity. B = 0.08 T, xenon 1.0 Aeq.

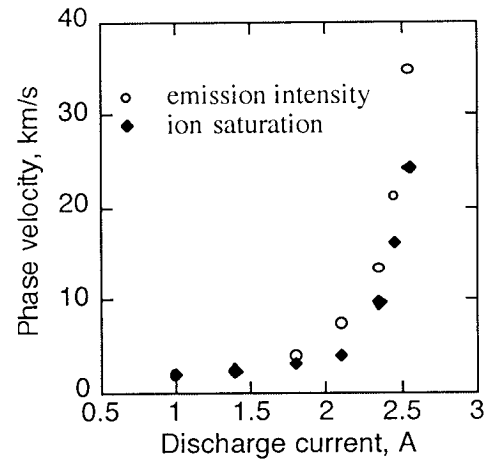

Fig. 11 Phase velocity of the waves in the emission intensity and in the ion saturation current. B = 0.08 T, xenon 1.0 Aeq.

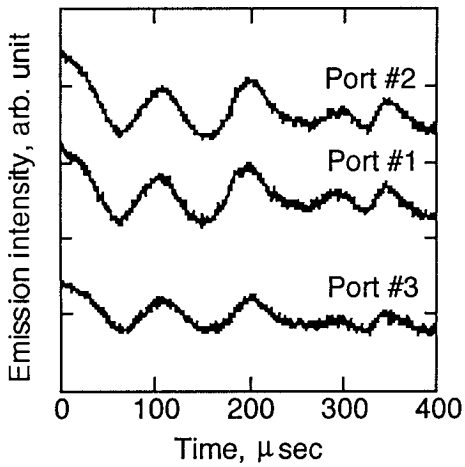

Fig. 12 Emission intensity oscillations measured at Ports #1, #2 and #3 (aligned in the axial direction.)

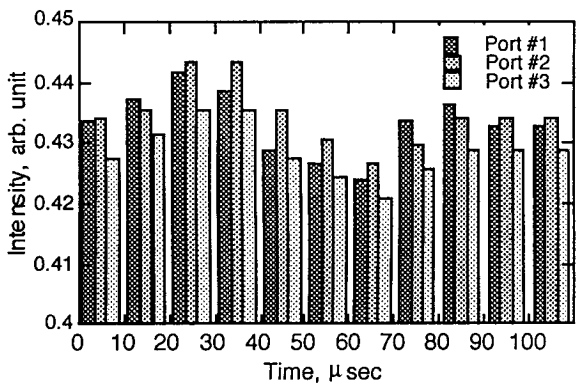

Fig. 13 Accumulated intensity variation. $I_d = 1.4$ A, $B =$ 0.08 T, xenon 1.0 Aeq.